

A Study on the Wireless Power Transfer Efficiency of Electrically Small, Perfectly Conducting Electric and Magnetic Dipoles

Charles L. Moorey¹ and William Holderbaum^{2, *}

Abstract—This paper presents a general theoretical analysis of the Wireless Power Transfer (WPT) efficiency that exists between electrically short, Perfect Electric Conductor (PEC) electric and magnetic dipoles, with particular relevance to near-field applications. The figure of merit for the dipoles is derived in closed-form, and used to study the WPT efficiency as the criteria of interest. The analysis reveals novel results regarding the WPT efficiency for both sets of dipoles, and describes how electrically short perfectly conducting dipoles can achieve efficient WPT over distances that are considerably greater than their size.

1. INTRODUCTION

Wireless Power Transfer holds the promise of delivering new and innovative charging solutions across a range of electronic applications, including medical implants [1, 2], consumer electronics [3, 4] and electric vehicles [5, 6]. However, the exponential decay of all electromagnetic fields with respect to increasing transfer distance means that WPT systems must be carefully designed in order to ensure that sufficient power reaches the desired end target. Mid-range WPT techniques have demonstrated that reasonably efficient WPT ($\approx 40\%$) can be achieved over distances of the order or several metres [7, 8]. Longer transmission distances can be achieved by using electromagnetic radiation [9] (typically in the form of either microwaves or laser beam), but this is at the cost of drastic reductions in the WPT efficiency. As such, this method of WPT is typically restricted to low-power energy harvesting [10, 11] applications rather than those involving dedicated transmitters and receivers, as in mid-range systems. There is therefore the need for further study in the field of WPT in order to improve upon both the efficiency of WPT and the distance for which efficient WPT can be achieved.

Electric and magnetic dipoles are fundamental objects in electromagnetic theory, and in the context of WPT can be used to achieve wireless transfer of power via magnetic induction, capacitive coupling or electromagnetic radiation. They are particularly relevant to the study of near-field and mid-range WPT systems as the transmitters and receivers of these systems are typically designed to be electrically small in order to exploit their high-efficiency near-field regions [7, 8]. However, electric and magnetic dipoles can also be used to model WPT systems involving more complicated transmitting/receiving structures. For example, Nam & Lee [12] showed that the electromagnetic behaviour of an electrically small, open ended helical antenna behaves like both an electric and a magnetic dipoles, emitting Transverse Electric (TE) and Transverse Magnetic (TM) TE_{10} and TM_{10} modes. Therefore better understanding of the WPT characteristics of electric and magnetic dipoles is important for the broad range of WPT systems that comprise both individual and multiple dipole elements.

Whilst WPT involving dipoles is relatively simple and well understood in the far-field (i.e., for radiative WPT), complexities arise in the near-field that motivate the need for further study. Previous

Received 23 June 2017, Accepted 8 August 2017, Scheduled 27 August 2017

* Corresponding author: William Holderbaum (W.Holderbaum@mmu.ac.uk).

¹ The University of Reading, Reading, UK. ² Manchester Metropolitan University, Science & Engineering, John Dalton Building, Manchester, UK.

studies involving electric and magnetic dipoles have used them to analyse near-field WPT between magnetostatic resonators [13], ferrite loop antennas [14], into dispersive tissue [15], in terms of their resonant frequency and geometric characteristics [16] and in the presence of metamaterial slabs [17, 18]. In contrast to previous work in the area, this paper presents a general theoretical analysis to study the WPT efficiency between electrically short, PEC electric and magnetic dipoles of equal size and orientation[†]. This is achieved by developing theoretical models for the dipoles and deriving their figure of merit in closed-form using their well-known electromagnetic field equations. In doing so, novel and useful results are revealed that to date have not yet been presented in the literature. In particular, it is revealed that the WPT efficiency is identical for both pairs of dipoles, and further, that this efficiency is independent of their characteristic geometric parameters. Our analysis uses the result of this independence to describe how use of electrically small, PEC dipoles can be used to achieve reasonably efficient WPT over distances that are much greater than their characteristic size.

In the next section, theoretical models for the dipoles are developed in order to derive the WPT efficiency and their figure of merit in closed form. The WPT efficiency is derived for two separate cases; one that considers the WPT efficiency between the dipoles in the absence of an output load at the receiving dipole (i.e., zero output impedance), and one that considers the WPT efficiency between the dipoles with a perfectly matched-load at the receiver. Consideration of the first case in Section 2.1.1 enables the fundamental power transfer that exists between the dipoles to be studied, which motivates their use as repeaters [19, 20] and is of interest to general applications of dipole coupling (e.g., EMI/EMC). It is also used later in the section to demonstrate how this near-field efficiency can be used to return the far-field efficiency for the dipoles under far field approximation, given by the Friis transmission equation and their gains. Consideration of the second case enables a theoretical upper bound for the efficiency to be defined, since it is maximised for when a perfectly matched load is connected to the receiver [8]. Section 3 analyses the WPT efficiency of the dipoles and discusses the key results, with conclusions of the work summarised in Section 4.

2. FORMULATION

This section uses a two-port network model in order to derive the two WPT efficiencies of the dipoles in terms the figure of merit, which is itself derived in terms of their self-resistances and the mutual impedance between them. Theoretical models of the dipoles are then developed in order to derive the self-resistances and mutual impedances required to formulate the figure of merit in terms of their frequency, separation distance and characteristic size.

2.1. Wireless Power Transfer Efficiency

In this section, two equations for the WPT efficiency between two coupled objects are derived; one in which there is no output load connected to the receiver (referred to as the “zero output impedance” case) and one in which a perfectly matched load is connected to the receiver. Derivation of the two cases enables the study of both the fundamental power transfer between the dipoles and the theoretical upper bound for the efficiency that exists when a perfectly matched load is connected to the receiver.

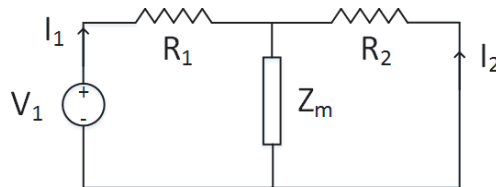


Figure 1. General two port network model describing the coupling between the dipoles.

[†] The effect of misalignment for near-field coupled small antennas was previously studied by Nam & Lee [12], and was therefore not considered in this analysis

2.1.1. Zero Output Impedance

First, the WPT efficiency between the dipoles with zero output impedance is derived. Figure 1 shows the general two port network model used to describe the coupling between the dipoles. Resonant operation is used to achieve high efficiency WPT, and the transmitter dipole has a resistance R_1 and the receiver dipole has a resistance R_2 . Both dipoles are connected through a lossless mutual impedance Z_m . The Circuit Theory equations for the two port network model shown in Figure 1 can be derived as Eqs. (1) and (2) [21]

$$V_1 = R_1 I_1 + Z_m I_2 \tag{1}$$

$$0 = R_2 I_2 + Z_m I_1 \tag{2}$$

where V_1 denotes the voltage supplied to the transmitter, and I_1 and I_2 denote the current in the transmitter and receiver respectively. Note that for non-resonant operation, the self-capacitances and self-inductances for the electric and magnetic dipoles respectively would need to be explicitly taken into account in Equations (1) and (2), as these would significantly alter the electromagnetic behaviour the systems. Considering first the case of the fundamental coupling between the dipoles, defined as the power transferred from the transmitter dipole to the receiver dipole in the absence of a receiver load, the receiver current, I_2 , can be written as Eq. (3)

$$I_2 = -\frac{Z_m I_1}{R_2} \tag{3}$$

The WPT efficiency, η , is then defined in terms of the power dissipated by the receiver (which is achieved through its radiative components under PEC approximation) through Eq. (4) as

$$\eta = \frac{|I_2|^2 R_2}{|I_1|^2 R_1 + |I_2|^2 R_2} \tag{4}$$

which through Equation (3) derives the WPT efficiency as (5)

$$\eta = \frac{1}{1 + \frac{R_1 R_2}{|Z_m|^2}} \tag{5}$$

It can be observed from Eq. (5) that the efficiency η is solely a function of the parameter $U = Z_m/\sqrt{R_1 R_2}$, which can be identified from [8] as the well known figure of merit, U , but derived in terms of Circuit Theory parameters. The WPT efficiency can therefore be written in terms of the figure of merit, U , as Eq. (6)

$$\eta = \frac{1}{1 + U^{-2}} \tag{6}$$

2.1.2. Perfectly Matched Load

Matched load operation is used to maximise the power transferred to a load connected in series with the receiving dipole, improving the overall efficiency of the system. The load is used to represent a useful output for the power, such as a battery or motor. Adding a matched load, R_{ML} , to the receiving dipoles modifies its resistance so that $R_2 \rightarrow R_2 + R_{ML}$. The matched load resistance is given in terms of the mutual impedance, Z_m , and the transmitter and receiver self-resistances R_1 and R_2 through Eq. (7) [21]

$$R_{ML} = \sqrt{R_1^2 + \frac{|Z_m|^2 R_1}{R_2}} \tag{7}$$

The matched load WPT efficiency was derived in terms of the figure of merit in [8], and is given by Eq. (8)

$$\eta_{ML} = \frac{U^2 \sqrt{1 + U^2}}{\left(1 + \sqrt{1 + U^2}\right) U^2 + \left(1 + \sqrt{1 + U^2}\right)^2} \tag{8}$$

2.2. Electric and Magnetic Dipoles

Electric and magnetic dipoles can be used to approximate the behaviour of electrically small, linear and circular single-turn, closed-loop geometries respectively. These objects are particularly useful to the study of near-field and mid-range WPT systems, in which the transmitters and receivers are often designed to be electrically small in order to exploit their high efficiency near-field regions [7, 8]. Typically, the dipole approximation is accurate for objects that are less than or equal to one-tenth of a wavelength in size; for the electric dipole the phrase size refers to its length and for the magnetic dipole this relates to its radius. Further approximations are also required in order to derive the electromagnetic field equations for both dipoles in closed form, and these are stated explicitly in Sections 2.2.1 and 2.2.2. The following sections proceed to develop the analytical formulation required to calculate the WPT efficiency between electrically small, PEC paired electric and magnetic dipoles.

2.2.1. Electric Dipole

This section proceeds to derive the figure of merit for the electric dipole in closed form using its well-known electromagnetic field equations.

Consider two electric dipoles of equal length l , oriented along the $+z$ axis in the xz -plane and separated by a distance r , as shown in Figure 2. Dipole 1, acting as the transmitter, is located at the centre of a spherical coordinate system, and dipole 2, acting as the receiver, is located at the point (x_2, z_2) , denoted in spherical coordinates as (r, θ) . Due to the symmetry around the z axis, the proceeding analysis is valid for any choice of the azimuthal angle, ϕ ($0 \leq \phi < 2\pi$). Assuming a time harmonic, constant current along the transmitter dipole oriented along the z -axis and of the form Eq. (9)

$$\mathbf{J}_1 = I_1 e^{i\omega t} \hat{\mathbf{z}} \quad (9)$$

this will induce a current, \mathbf{J}_2 , along the receiving dipole of the form (10)

$$\mathbf{J}_2 = I_2 e^{i(\omega t - \beta r)} \hat{\mathbf{z}} \quad (10)$$

where in Equations (9) and (10) I_1 and I_2 are real constants representing the current amplitudes on the transmitter and receiver dipoles respectively, ω represents the angular frequency, β denotes the free-space wavenumber, the term $e^{i\beta r}$ represents the propagation delay due to the finite speed of electromagnetic fields of the transmitting dipole and $\hat{\mathbf{z}}$ is the unit vector along the z -axis.

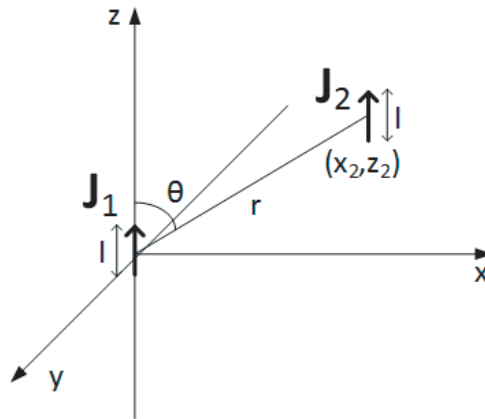


Figure 2. System comprising two identically sized and oriented electric dipoles.

Power is transferred between the dipoles through their mutual impedance Z_m , which can be calculated using the induced emf method in Eq. (11) [22]

$$Z_m = \frac{1}{I_1 I_2} \int \mathbf{E}_1 \cdot \mathbf{J}_2 dl_2 \quad (11)$$

where \mathbf{E}_1 denotes the electric field of the transmitter dipole, and dl_2 is the line element of the receiver dipole. Making the assumption that the dipoles are electrically small, i.e., $l \ll \lambda$, and further that $r \gg l$, the electric fields of the transmitting dipole at the receiver can be written in spherical coordinates as Eqs. (12) and (13) [23, Ch. 10, 294–296]

$$E_r(r, \theta) = -\frac{iI_1 l \cos \theta}{2\omega\pi\epsilon_0 r^3} (1 + i\beta r) e^{i(\omega t - \beta r)} \quad (12)$$

$$E_\theta(r, \theta) = -\frac{iI_1 l \sin \theta}{4\pi\epsilon_0 \omega r^3} (1 + i\beta r - (\beta r)^2) e^{i(\omega t - \beta r)} \quad (13)$$

where ϵ_0 the permittivity of free-space. Using Equations (12) and (13), and assuming that the spatial variation of the electric fields of the transmitter dipole along the length of the receiving dipole are negligibly small, the mutual impedance can be derived as

$$Z_m = \frac{-il^2}{4\pi\omega\epsilon_0 r^3} \left(\frac{1}{2} \sin^2 \theta (1 + i\beta r - (\beta r)^2) - \cos^2 \theta (1 + i\beta r) \right) e^{-i\beta r} \quad (14)$$

Calculation of the figure of merit also requires calculation of the self-resistance of the dipoles, which under PEC approximation is solely their radiation resistance of Eq. (15) [23, Ch. 11, 297]

$$R = \frac{\mu_0(\omega l)^2}{6\pi c} \quad (15)$$

where μ_0 and c are the free-space permeability and the speed of light respectively. Given that the dipoles are identical, their self-resistances are equal so that $R_1 = R_2 = R$. Using Equations (14) and (15), the figure of merit for the dipoles, U_e , can be derived as Eq. (16)

$$U_e = \frac{3}{2} \frac{1}{\beta^3 r^3} \left(\frac{1}{4} \sin^4 \theta (1 - \beta^2 r^2 + \beta^4 r^4) + \cos^4 \theta (1 + \beta^2 r^2) - \sin^2 \theta \cos^2 \theta \right)^{1/2} \quad (16)$$

2.2.2. Magnetic Dipole

Having derived the figure of merit for coupled electric dipoles in the previous section, this section proceeds to derive the figure of merit for coupled, identical magnetic dipoles.

Figure 3 shows two magnetic dipoles, of equal radius a , and once again embedded in a spherical coordinate system such that the receiving dipole (dipole 2) is located at an angle θ and a distance r away from the transmitter dipole (dipole 1). A current of $\mathbf{J}_1 = I_1 e^{i\omega t} \hat{\phi}$ is assumed along the transmitter dipole, which subsequently induces the current $\mathbf{J}_2 = I_2 e^{i\omega t - \beta r} \hat{\phi}$ in the receiver (with $\hat{\phi}$ representing the unit vector of the azimuthal angle, ϕ). The normals to the surfaces of each of the dipoles, $\hat{\mathbf{n}}_1$ and $\hat{\mathbf{n}}_2$, are aligned to the $+z$ axis. Whilst it is possible to use the induced emf method in Eq. (11) to calculate

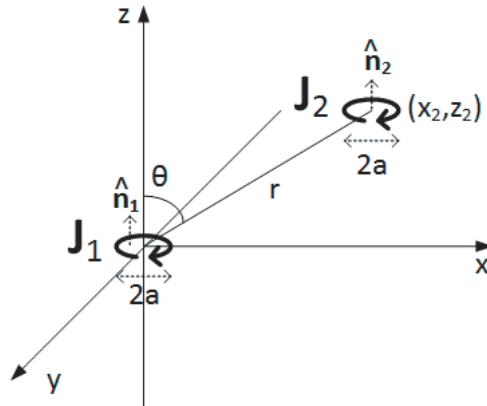


Figure 3. System comprising two identically sized and oriented magnetic dipoles.

the mutual impedance between the magnetic dipoles, their circular geometries leads to unnecessary complication, and so Faraday's law of induction is used instead. Faraday's law gives the magnetic flux, Φ_m , through the surface of the receiving dipoles, S_2 , in terms of the magnetic field of transmitting dipole, \mathbf{H}_1 , incident upon the surface of the receiver as Eq. (17) [24, Ch. 6, 218]

$$\Phi_m = \mu_0 \iint_{S_2} \mathbf{H}_1 \cdot d\mathbf{s}_2 \quad (17)$$

where $d\mathbf{s}_2 = ds\hat{\mathbf{n}}_2$ denotes the surface element of receiver dipole, enclosed by its current, \mathbf{J}_2 . Making the assumption that the magnetic dipoles are electrically small, i.e., $a \ll \lambda$, and further that $r \gg a$, the magnetic fields the transmitter dipole are given by Equations (18) and (19) [25]:

$$H_r = \frac{I_1 a^2 \cos \theta}{2r^3} (1 + i\beta r) e^{i(\omega t - \beta r)} \quad (18)$$

$$H_\theta = \frac{I_1 a^2 \sin \theta}{4r^3} (1 + i\beta r - (\beta r)^2) e^{i(\omega t - \beta r)} \quad (19)$$

The mutual inductance, L_m , between the dipoles is related to the magnetic flux Φ_m through Eq. (20) [24, Ch. 6, 232]

$$L_m = \frac{\Phi_m}{I_1} \quad (20)$$

Using Equations (17)–(20), and assuming the spatial variation of the magnetic fields of the transmitter dipole to be small over the surface of the receiving dipole, the mutual inductance between the magnetic dipoles is derived as Eq. (21)

$$L_m = -\frac{\mu_0 \pi a^4}{4r^3} \left(\frac{1}{2} \sin^2 \theta (1 + i\beta r - (\beta r)^2) - \cos^2 \theta (1 + i\beta r) \right) e^{-i\beta r} \quad (21)$$

which gives the inductive mutual impedance, Z_m , between the magnetic dipoles as Eq. (23)

$$Z_m = i\omega L_m \quad (22)$$

$$Z_m = -\frac{i\mu_0 \omega \pi a^4}{4r^3} \left(\frac{1}{2} \sin^2 \theta (1 + i\beta r - (\beta r)^2) - \cos^2 \theta (1 + i\beta r) \right) e^{-i\beta r} \quad (23)$$

Since the sizes of the magnetic dipoles are equal, so are their self-resistances so that $R_1 = R_2 = R$. Under PEC approximation, the self-resistance of the magnetic dipoles is solely their radiation resistance of Eq. (24)

$$R = \frac{\mu_0 (\omega a)^4 \pi}{6c^3} \quad (24)$$

Using Equations (23) and (24), the figure of merit of the magnetic dipoles, U_m , can be derived as Eq. (25)

$$U_m = \frac{3}{2} \frac{1}{\beta^3 r^3} \left(\frac{1}{4} \sin^4 \theta (1 - \beta^2 r^2 + \beta^4 r^4) + \cos^4 \theta (1 + \beta^2 r^2) - \sin^2 \theta \cos^2 \theta \right)^{1/2} \quad (25)$$

which is identical to the figure of merit that was derived for the electric dipoles in Eq. (16). This result shows that the WPT efficiency between coupled electric and magnetic dipoles is identical when they are electrically short and perfectly conducting. Whilst this equivalence is known in the far-field through the use of the Friis transmission equation and the gains of the dipoles, it has not yet been shown for shorter separation distances. This is an important result as it reveals there can be flexibility in the design of WPT systems involving electrically short, PEC dipoles where efficiency is the main focus. To simplify further analysis, the notation in Eq. (26)

$$U = U_e = U_m \quad (26)$$

is adopted.

2.3. Link to the Far-Field WPT Efficiency

This section shows how the far-field efficiency for the dipoles, which can be derived using the Friis transmission equation and their gains, can be similarly derived using the figure of merit and the efficiency, η , given by Equation (6).

Using Equation (16), the square of the figure of merit of the dipoles can be re-written as

$$U^2 = \frac{9}{4} \frac{1}{\beta^6 r^6} \left(\frac{1}{4} \sin^4 \theta (1 - \beta^2 r^2 + \beta^4 r^4) + \cos^4 \theta (1 + \beta^2 r^2) - \sin^2 \theta \cos^2 \theta \right) \quad (27)$$

Under far-field approximation, $\beta r \gg 1$, the term in $(\beta r)^{-2}$ dominates such that the figure of merit for the dipoles in the far-field, U_{far} , can be approximated by

$$U_{far} \approx \frac{3 \sin^2 \theta}{4 \beta r} \quad (28)$$

In the far-field, the WPT efficiency is typically low as the majority of power is dissipated into free-space, with only a small fraction reaching the desired end-target. Therefore over these distances, $|Z_m| \ll R_{rad}$ and the parameter U^{-2} in the equation for the efficiency η in Eq. (6) becomes large, i.e., $U^{-2} \gg 1$. Under this condition, the far-field efficiency, η_{far} can be reasonably approximated as

$$\eta_{far} \approx U_{far}^2 \quad (29)$$

$$= \frac{9 \sin^4 \theta}{16 \beta^2 r^2} \quad (30)$$

which can be re-written as Eq. (31)

$$\eta_{far} = \left(\frac{\lambda}{4\pi r} \right)^2 \left(\frac{3}{2} \sin^2 \theta \right) \left(\frac{3}{2} \sin^2 \theta \right) \quad (31)$$

from which the gain of the dipoles, $G = 3 \sin^2 \theta / 2$ [26], can be identified, such that Equation (31) can be written as Eq. (32)

$$\eta_{far} = \left(\frac{\lambda}{4\pi r} \right)^2 G^2 \quad (32)$$

which can be recognised as the well-known Friis transmission equation [26], which describes the far-field WPT efficiency between two electromagnetic objects. Therefore, the theoretical models developed in the previous sections for the dipoles can be used to analyse their WPT efficiency for both near-field and far field distances (whilst observing the approximations noted Sections 2.2.1 & 2.2.2), allowing an almost spatially unrestricted analysis of the dipoles to be undertaken.

3. ANALYSIS & DISCUSSION

This section uses the equations derived in the previous section to analyse the WPT efficiency derived for dipoles and discusses the key results.

Figure 4 plots Equations (8) and (6) (which represent the WPT efficiencies with and without a perfectly matched load at the receiver respectively) in terms of the figure of merit, U . The graph shows the proportionality that exists between both efficiencies with respect to the figure of merit, with efficiencies of 90% and above possible for both cases for $U \geq 40$. Therefore in order to improve the WPT efficiency of the dipoles, efforts should be made towards increasing the figure of merit. Figure 4 also shows that for a given figure of merit, U , the WPT efficiency of the dipoles with a perfectly matched output load at the receiver is always less than the WPT efficiency when the load is absent. Given that a perfectly matched load is defined as the load value that maximises the efficiency of power transfer to it, this result implies that an output load, either perfectly matched or otherwise, is not able to extract all of the power that would be delivered to the receiver if the output load was absent.

Inspection of the derived figure of merit for the dipoles in Eq. (25) reveals that it is invariant with respect to the size of the dipoles, i.e., there is no dependence on the characteristic dimensions l or a of

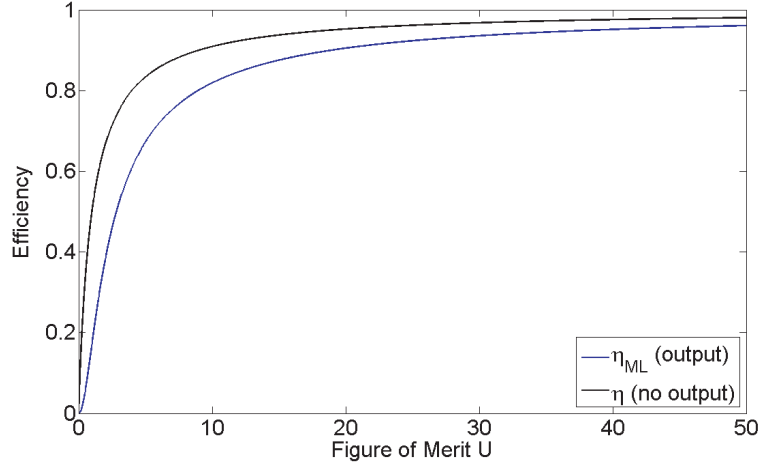


Figure 4. The variation in the WPT efficiencies η and η_{ML} with respect to the figure of merit, U .

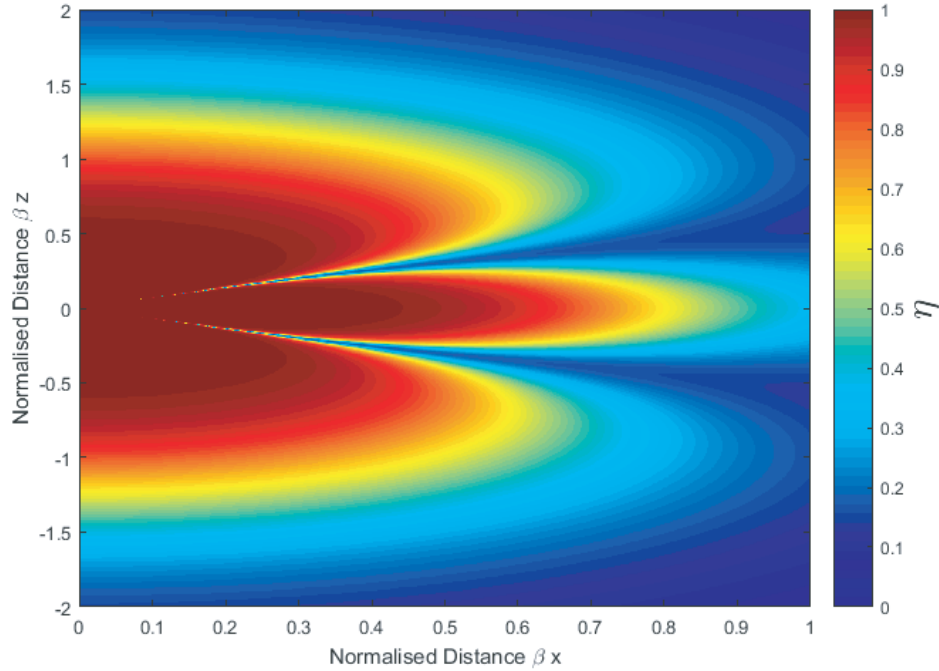


Figure 5. Spatial variation in the WPT efficiency, η , between coupled electric and magnetic dipoles with zero output impedance. The x and z coordinate axes are normalised with respect to the wavelength λ .

the dipoles. Once again, whilst this result is known in the far-field through the gains of the dipoles, it has not yet been shown for shorter separation distances. This is also a useful result as it reveals that the size of the dipoles can be increased or decreased without changing the efficiency, important in WPT systems where there are size constraints.

Figures 5 and 6 plot the spatial variation in the WPT efficiency in the xz -plane of the dipoles (see Figures 2 and 3) using Equations (6) and (8) respectively. The distances x and z for both plots have also been normalised with respect to the angular wavelength λ through the wavenumber $\beta = 2\pi/\lambda$, in order to enable analysis that is general in terms of the frequency. Figures 5 and 6 reveal the difference between the two efficiencies, with the zero output impedance case achieving higher efficiencies across range than the case involving a perfectly matched load. For example, at a distance of $\beta z = 1$ along the z -axis

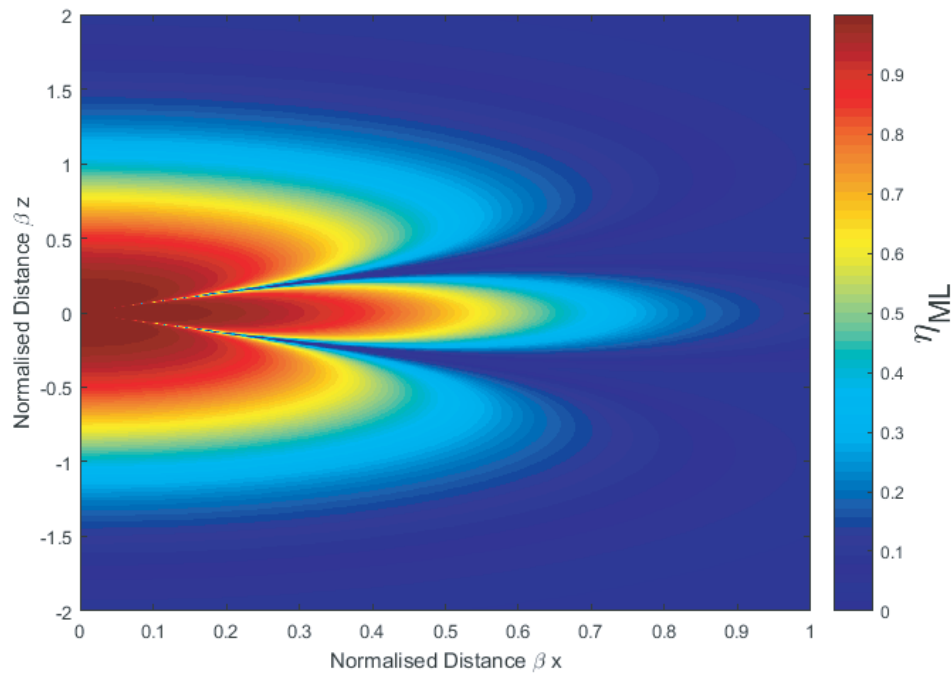


Figure 6. Spatial variation in the WPT efficiency, η_{ML} , between coupled electric and magnetic dipoles with an output load connected to the receiver dipole. The x and z coordinate axes are normalised with respect to the wavelength λ .

($x = 0$), Figure 5 shows the efficiency between the dipoles is almost 82%, whereas Figure 6 at the same distance shows the efficiency is approximately 40%, which is reduction of over 50%. Similarly, along the x -axis ($z = 0$) for a distance of $\beta x = 1$ the difference between the two efficiencies is approximately 24%. The efficiency of transfer that exists between the dipoles when an output load is absent for the distances shown in Figure 5 motivate the use of the dipoles as repeaters [19, 20] (which are not serially loaded) in order to utilise these efficiencies and significantly increase the distance of efficient WPT. Further, the results shown in Figure 5 are also of interest to more general applications involving dipole coupling outside of WPT, such as the study of EMI/EMC effects.

In order to illustrate the practical importance of the invariance of the efficiency of the dipoles with respect to their size, consider two dipoles of length/radius of 0.1λ separated along the z axis by a normalised distance $\beta z = 1$. This normalised distance is equal to a distance along the z -axis that is 1.59 times the length of the dipole. At this distance the efficiency $\eta_{ML} = 40.2\%$, which is low considering that efficiencies of this value have been achieved for distances that are 8 times the size of the transmitter/receivers used [27]. However, reducing the size of the dipoles to $l = 0.01\lambda$ and operating over the same transmission distance yields the same efficiency (since the efficiency has been shown to be independent of the size of the dipoles), but over a distance that equates to 15.92 times the size of the dipoles involved, which is almost double that which is typically reported in the literature for near-field, mid-range WPT. This a favourable result as it offers the possibility of downsizing the dipoles whilst still achieving significant operating distances, relative to their size. Whilst there are practical challenges associated with achieving almost PEC-like behaviour, a number of examples exist in the literature where the results of this analysis have direct implications; for example, for WPT systems involving highly conducting materials such as graphene [28] or superconductors [29, 30]. It is further worth noting that where this analysis is being used as the foundation to model more complicated geometries (such as coils or helical antennas for example), factors such as leakage inductance, parasitic capacitance and the proximity effect increasingly modify the behaviour of the system and should therefore be taken into account. However, since these factors are vary significantly depending on the geometry in question, they are beyond the scope of the general analysis presented in this paper.

4. CONCLUSION

This paper has considered the WPT efficiency between electrically short PEC electric and magnetic dipoles of equal size and orientation. This was achieved by deriving the figure of merit in closed form for the dipoles, which to date has not yet been presented in the literature. Two cases of WPT have been considered; The first case considered the WPT efficiency of the dipoles with zero output impedance (i.e., with no output load connected to the receiver), and the second case considered the WPT efficiency with a perfectly matched load serially connected to the receiver. This enabled the effect associated with the presence of a matched load to be considered, and further how the near-field models developed for the dipoles returned their well-known far-field efficiency (given by the Friis equation) under far-field approximation. Further, the analysis also showed that the WPT efficiency between paired electric dipoles was equivalent to the WPT efficiency of paired magnetic dipoles, and that this efficiency was independent of their characteristic geometric parameters. This result was extended to consider how electrically short, PEC dipoles could achieve efficient WPT over near-field distances considerably greater than their size and improving upon of what is typically reported in the literature in this regard.

REFERENCES

1. Ramrakhyani, A. K., S. Member, and S. Mirabbasi, "Design and optimization of resonance-based efficient wireless power delivery systems for biomedical implants," *IEEE Transactions on Biomedical Circuits and Systems*, Vol. 5, No. 1, 48–63, 2011.
2. Kiani, M., U.-M. Jow, and M. Ghovanloo, "Design and optimization of a 3-coil inductive link for efficient wireless power transmission," *IEEE Transactions on Biomedical Circuits and Systems*, Vol. 99, No. 6, 1, Jul. 2011.
3. Choi, J., Y.-H. Ryu, D. Kim, N. Y. Kim, C. Yoon, Y.-k. Park, and S. Kwon, "Design of high efficiency wireless charging pad based on magnetic resonance coupling," *9th European Radar Conference (EuRAD)*, 590–593, 2012.
4. Wu, P., F. Bai, Q. Xue, X. Liu, and S. Y. R. Hui, "Use of frequency-selective surface for suppressing radio-frequency interference from wireless charging pads," *IEEE Transactions on Industrial Electronics*, Vol. 61, No. 8, 3969–3977, 2014.
5. Eberle, W. and F. Musavi, "Overview of wireless power transfer technologies for electric vehicle battery charging," *IET Power Electronics*, Vol. 7, No. 1, 60–66, Jan. 2014.
6. Li, S. and C. Mi, "Wireless power transfer for electric vehicle applications," *IEEE Journal of Emerging and Selected Topics in Power Electronics*, Vol. Pp, No. 99, 1, 2014.
7. Park, C., S. Member, S. Lee, G.-H. Cho, S. Member, C. T. Rim, and A. O. C. Configuration, "Innovative 5-m-off-distance inductive power transfer systems with optimally shaped dipole coils," *IEEE Transactions on Power Electronics*, Vol. 30, No. 2, 817–827, 2015.
8. Kurs, A., A. Karalis, R. Moffatt, J. D. Joannopoulos, P. Fisher, and M. Soljacic, "Wireless power transfer via strongly coupled magnetic resonances," *Science*, Vol. 317, No. 5834, 83–85, New York, N.Y., Jul. 2007.
9. Brown, W. C., "The history of wireless power transmission," *Solar Energy*, Vol. 56, No. 1, 3–21, 1996.
10. Huang, L., V. Pop, R. de Francisco, R. Vullers, G. Dolmans, H. de Groot, and K. Imamura, "Ultra low power wireless and energy harvesting technologies — An ideal combination," *2010 IEEE International Conference on Communication Systems*, 295–300, Nov. 2010.
11. Popovic, Z., E. A. Falkenstein, D. Costinett, and R. Zane, "Low-power far-field wireless powering for wireless sensors," *Proceedings of the IEEE*, Vol. 101, No. 6, 1397–1409, 2013.
12. Lee, J. and S. Nam, "Fundamental aspects of near-field coupling small antennas for wireless power transfer," *IEEE Transactions on Antennas and Propagation*, Vol. 58, No. 11, 3442–3449, 2010.
13. Mur-miranda, O., G. Fantì, Y. Feng, K. Omanakuttan, R. Ongie, A. Setjoadi, and F. W. Olin, *Wireless Power Transfer Using Weakly Coupled Magnetostatic Resonators*, 4179–4186, 2010.

14. Warnick, K., B. Gottula, S. Shrestha, and J. Smith, "Optimizing power transfer efficiency and bandwidth for near field communication systems," *IEEE Transactions on Antennas and Propagation*, Vol. 61, No. 2, 927–933, 2013.
15. Poon, A., S. O'Driscoll, and T. Meng, "Optimal frequency for wireless power transmission into dispersive tissue," *IEEE Transactions on Antennas and Propagation*, Vol. 58, No. 5, 1739–1750, May 2010.
16. Moorey, C., W. Holderbaum, and B. Potter, "Investigation of high-efficiency wireless power transfer criteria of resonantly-coupled loops and dipoles through analysis of the figure of merit," *Energies*, Vol. 8, No. 10, 11 342–11 362, 2015.
17. Urzhumov, Y. and D. Smith, "Metamaterial-enhanced coupling between magnetic dipoles for efficient wireless power transfer," *Physical Review B*, Vol. 83, No. 20, 1–23, 2011.
18. Lipworth, G., J. Ensworth, K. Seetharam, D. Huang, J. S. Lee, P. Schmalenberg, T. Nomura, M. S. Reynolds, D. R. Smith, and Y. Urzhumov, "Magnetic metamaterial superlens for increased range wireless power transfer," *Scientific Reports*, Vol. 4, 3642, 2014.
19. Zhong, W., C. K. Lee, and S. Y. Ron Hui, "General analysis on the use of tesla's resonators in domino forms for wireless power transfer," *IEEE Transactions on Industrial Electronics*, Vol. 60, No. 1, 261–270, 2013.
20. Ahn, D. and S. Hong, "A study on magnetic field repeaters in wireless power transfer," *IEEE Transactions on Industrial Electronics*, Vol. 60, No. 1, 360–371, 2013.
21. Garnica, J., J. Casanova, and J. Lin, "High efficiency midrange wireless power transfer system," *2011 IEEE MTT-S International Microwave Workshop Series on Innovative Wireless Power Transmission: Technologies, Systems, and Applications (IMWS)*, No. 5, 73–76, 2011.
22. Orfanidis, S. J., *Electromagnetic Waves and Antennas*, Online, New Jersey, 2014.
23. Hammond, P., *Applied Electromagnetism*, Pergamon Press, New York, 1971.
24. Grant, I. S. and W. R. Phillips, *Electromagnetism*, 3rd Edition, John Wiley & Sons, 2003.
25. Li, L.-W., M.-S. Leong, P.-S. Kooi, and T.-S. Yeo, "Exact solutions of electromagnetic fields in both near and far zones radiated by thin circular-loop antennas: A general representation," *IEEE Transactions on Antennas and Propagation*, Vol. 45, No. 12, 1741–1748, 1997.
26. Drabowitch, S., A. Papiernik, H. Griffiths, and J. Encinas, *Modern Antennas*, Chapman and Hall, 1998.
27. Karalis, A., J. Joannopoulos, and M. Soljačić, "Efficient wireless non-radiative mid-range energy transfer," *Annals of Physics*, Vol. 323, No. 1, 34–48, Jan. 2008.
28. Dragoman, M., M. Aldrigo, A. Dinescu, D. Dragoman, and A. Costanzo, "Towards a terahertz direct receiver based on graphene up to 10 THz," *Journal of Applied Physics*, Vol. 115, No. 4, 044307, Jan. 2014.
29. Zhang, G., H. Yu, L. Jing, J. Li, Q. Liu, and X. Feng, "Wireless power transfer using high temperature superconducting pancake coils," *IEEE Transactions on Applied Superconductivity*, Vol. 24, No. 3, 3–7, 2013.
30. Sedwick, R. J., "Long range inductive power transfer with superconducting oscillators," *Annals of Physics*, Vol. 325, No. 2, 287–299, Feb. 2010.